Magazine of Civil Engineering

ISSN 2712-8172

journal homepage: http://engstroy.spbstu.ru/

Research article

UDC 624.139.22

DOI: 10.34910/MCE.120.9

Regression models of irregular vertical displacement of a roadway cross section caused by frost heaving

V.S. Churilin , ***O.V. Matvienko***, ***V.N. Efimenko***, ***S.V. Efimenko***

Tomsk State University of Architecture and Building, Tomsk, Russian Federation

lex-16-2008@mail.ru

Keywords: frost heaving, air-freezing, thermal resistance of pavement, pavement displacement, regression model

Abstract. Subgrade clay is subjected to frost heaving under the effect of cold air and adequate soil moisture. The existing prediction models for frost heaving have a number of drawbacks: they are complicated for practical use and unable to evaluate irregular vertical displacements. Winter monitoring of 14 road sections was performed to evaluate irregular vertical displacement of pavement surface cross section under the action of frost heaving. The obtained data on vertical displacement of points were processed using mathematical statistics methods, and predictive regression models were built for vertical displacement of pavement during winter season. Stable relations were defined between displacement of points on the broken line (center-line of a road) and the factors including air-freezing index, thermal resistance of pavement, impact of subsurface water on frost heave, the pressure of pavement on the subgrade surface. Adequacy of the built models was checked using the results of displacement of points on the pavement surface within test sections. The first check concerned comparison of the values of modeling of the average displacement of points on the broken line caused by frost heaving, where mean absolute error was up to 20 %. For the case of close occurrence of subsurface water, the model prediction of the average displacement of points on the broken line showed significant difference from the actually recorded values. The second check concerned the displacement of points on the pavement in relation to displacement of points on the broken line, with the mean absolute value of up to 13 %.

Funding: FEMN-2022-0003 of the Ministry of Science and Higher Education of the Russian Federation

Acknowledgments: The authors thank the anonymous reviewers, whose comments helped to improve the quality of this paper. The authors would like to acknowledge Shannon Fiecke, Benjamin Worrell, and Sandy McCully the Department of transportation Minnesota for the information provided. My thanks are due to our Italian colleague Lucia Tsantilis for her help.

Citation: Churilin, V.S., Matvienko, O.V., Efimenko, V.N., Efimenko, S.V. Regression models of irregular vertical displacement of a roadway cross section caused by frost heaving. Magazine of Civil Engineering. 2023. 120(4). Article no. 12009. DOI: 10.34910/MCE.120.9

1. Introduction

Phase change of water in clay soil in cold climate regions (according to the climate classification by Köppen-Geiger [1]) causes significant pavement defects and increase of repair costs [2–4]. When subgrade soil freezes, the water in it starts migrating and transits from liquid to solid state, thus leading to displacement of pavement surface, or frost heaving. The study performed by Taber [5] highlights that the main reason of frost heaving is ice segregation in the subgrade soil caused by mass transfer (of water) to the cooling region. In 1929, Taber performed an experiment with freezing soil samples saturated with benzene (the latter contracts as it freezes) which enabled him to conclude that volume expansion of pore

water while freezing in soil is not related to the main mechanism of frost heaving. S. Taber's vision of the reasons of mass transfer to the cooling region has been improved in the research by Beskow [6] and other studies. In 1937, Tsytovich [7] formulated the concept of moisture redistribution, which found scientific consensus.

Today, studies on physical causes of ice segregation, influencing factors and their combination, as well as their impacts on engineering structures are still ongoing [8, 9]. Fig. 1 shows the development of research on frost heaving of soil. The qualitative parameter of publications shows an annual growth, which demonstrates the relevance of the topic of soil frost heaving and its effect on engineering structures.

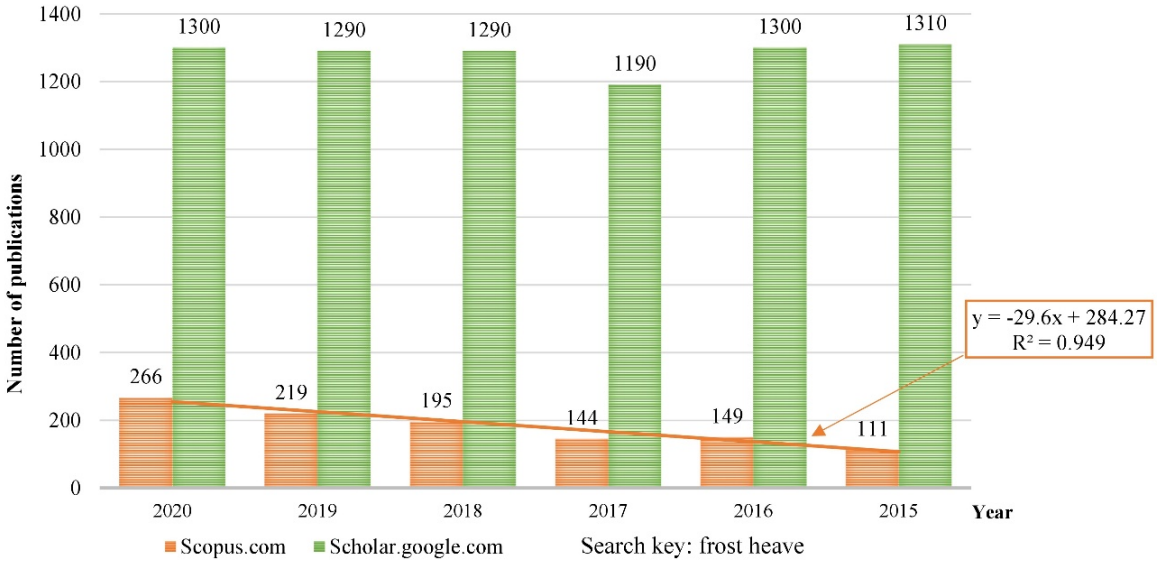

Figure 1. Variation of the number of publications on frost heaving (based on scopus.com and scholar.google.com data as of January 2021).

Studies on physical mechanisms, chemical and thermodynamic processes in frozen subgrade soil are the basis for building predictive models of frost heaving of soil.

A comprehensive description of predictive model building and development forsoil frost heaving is provided in the review carried out by Black [10]. Other studies that are worth to mention include research works that consider heat transfer through isotopic medium [11, 12] and the secondary frost heaving theory developed in 1985 by O'Neill and Miller [13]. These studies made a considerable contribution to the understanding and prediction of frost heaving of soil. Recent investigations suggest the adoption of both traditional and innovative approaches that can be used to model the frost heaving process [14–17].

The study performed by Jing et al. in 2021 [18] is worth noting for providing a prediction of longitudinal strains occurring in the railway subgrade under the action of frost heave by using the Artificial Intelligence (AI) technology, namely Artificial Neural Network (ANN) and Long-Short Term Memory (LSTM). The frost heave prediction made for a 10-day period with the use of the LSTM model of a single-layer neural network revealed good agreement between the modeling and full-scale experiment results. Eighty percent of the data obtained during the monitoring were used for training of the neural network, while twenty percent were applied in the network testing. The LSTM model was tested using the full-scale monitoring results obtained for the railway sections and used for its training. This may not be representative of the frost heave pattern on other railway sections taking into account variation of railway subgrade freezing conditions. The prediction of frost heave for the entire period is necessary for the model to be applicable for practical use. This aspect implies that a high computing capacity is needed.

Despite the actual achievements in frost heaving prediction, difficulties were found in performing practical comparison between the above-mentioned models and their applications. The problem of irregular vertical displacements of the pavement surface caused by frost heaving cannot be easily solved by using most of mathematical models. Complex specialized equipment and highly trained professionals are required to obtain soil parameters used for modeling.

The goal of this study is the development of a regression model for predicting irregular vertical displacement of pavements in crosswise direction under the action of frost heaving. The model will serve as an available solution for road engineers. The factors selected for the regression analysis take into consideration not only the relevance for the frost heaving phenomenon but also the availability of data for road engineers.

2. Materials and Methods

Monitoring of the pavement surface displacement during winter season was performed for model building purposes. Studies of soil conditions were carried out for the road network in the area in question (geolocation data of the monitored sections are provided in the paper appendix). The area is characterized by excessive moisture and deep seasonal freezing. The frost depth from the clean surface of subgrade soil in the studied area by early spring is approximately 200 to 220 cm, and in certain years it reaches 260 cm. Vast areas covered with swamps and forest have significant impact on the moisture content in soil and affect mass transfer in subgrade soils of roadways in the area under study [19]. Soil samples were taken along the curb of the roadway from the sections selected for monitoring (Fig. 2) to be tested in the laboratory. Trial holes were designed on the selected sections in order to specify structural solutions.

Figure 2. Location of sections for monitoring of pavement displacement in the area under study.

Table 1 presents the overview of laboratory test results for soils from the sections of operating roadways selected for monitoring.

Table 1. The results of laboratory tests of soil samples.

Number of section	Classification of soil according to Unified Soil Classification System [20]	Particle density, g/cm^3 (kN/m^3) [21]	Natural moisture content, % [21]	Plastic limit [22]	Liquid limit [22]	Plasticity index [22]	Liquidity index [23]
1	Lean clay	2.74 (26.87)	18.93	18	30	12	stiff
2	Lean clay	2.64 (25.89)	21.76	21	37	16	stiff
3	Lean clay	2.71 (26.58)	19.64	19	27	8	stiff
4	Lean clay	2.68 (26.28)	17.93	23	38	15	very stiff
5	Lean clay	2.77 (27.16)	18.95	22	37	15	stiff
6	Lean clay	2.72 (26.67)	21.38	24	32	8	very stiff
7	Lean clay	2.72 (26.67)	20.28	19	31	12	stiff
8	Lean clay	2.60 (25.50)	22.35	20	33	13	stiff
9	Lean clay	2.68 (26.28)	25.00	22	30	8	firm-stiff
10	Lean clay	2.78 (27.26)	19.80	18	35	17	stiff
11	Lean clay	2.66 (26.09)	22.19	20	32	12	stiff
12	Lean clay	2.75 (26.97)	15.96	17	31	14	very stiff
13	Lean clay	2.54 (24.91)	23.00	28	40	12	very stiff
14	Lean clay	2.65 (25.99)	24.40	18	32	14	firm-stiff

Subgrade soils of the roadway sections selected for monitoring of pavement displacement belong to lean clay [20]. The values of plastic limit vary between 17 and 28, while the values of liquid limit belong to the range from 27 to 40 (Table 1). Soil samples taken from the road sections were subjected to hydrometer grain size analysis. Fig. 3 illustrates the final grain-size distributions.

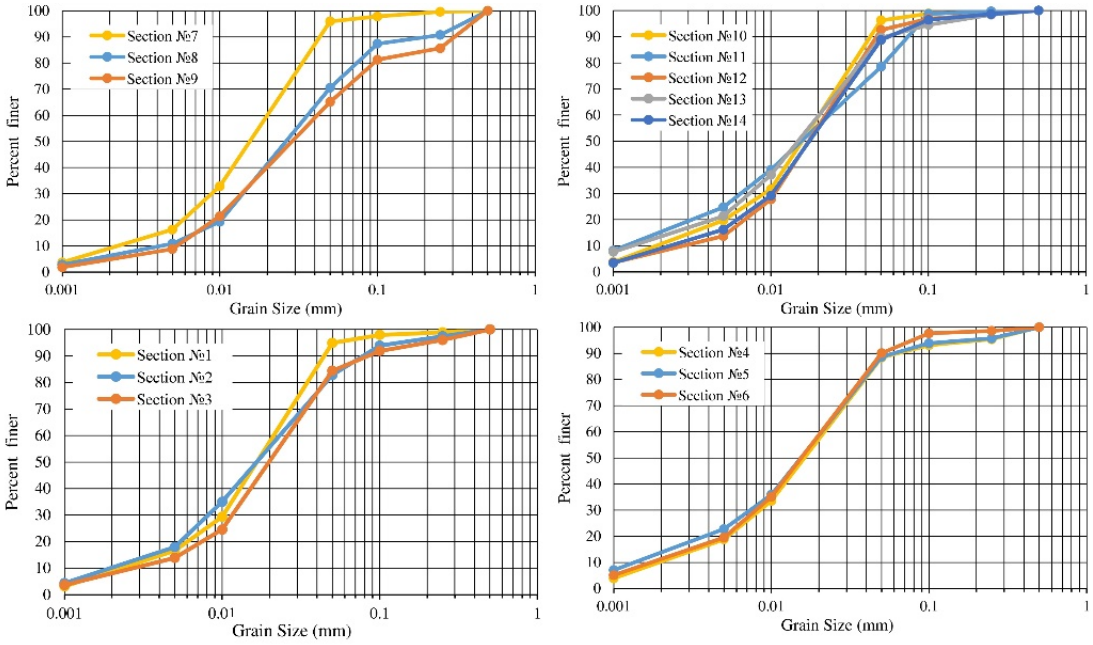

Figure 3. Grain-size distributions for the tested soils.

Normally, soils that belong to the same class and have similar grain-size composition show similar heaving properties in the same testing conditions. This observation is confirmed by the outcomes of laboratory tests performed to define the relative frost heave. The results of these tests are presented in Table 2. In laboratory conditions, relative frost heave was defined with freely supplied water in two freeze-thaw cycles at a temperature of –6 °C in the freezing chamber. The soil sample was 15.5 cm high and 10 cm in diameter [24].

Table 2. The results of laboratory tests of relative frost heave.

No. of section	Bulk density, g/cm^3	Relative frost heave
1	2.10	0.0407
2	2.11	0.0409
3	2.11	0.0403
4	2.13	0.0415
5	2.10	0.0388
6	2.14	0.0416
7	2.05	0.0389
8	2.11	0.0402
9	2.10	0.0406
10	2.10	0.0403
11	2.03	0.0389
12	2.12	0.0386
13	2.04	0.0388
14	2.10	0.0405

Note: the table contains average values out of the testing campaign. The campaign consisted of two laboratory tests of the same type of soil sampled from the subgrade of the corresponding section for pavement displacement monitoring.

The test results obtained for relative frost heave vary around the average value of 0.0400 within ±4 %. Besides, one should note the impact of the content of exchangeable cations containing ions of Ca^{2+}, Mg^{2+} and Na^{+} in montmorillonite, kaolinite and illite minerals that affect the heaving properties of clay soil. In the area under study, the total content of exchangeable cations of Ca^{2+}, Mg^{2+} in soil is ≈ 5.2 times higher than that of Na^{+} [25]. Darrow and Ross [26] estimated the impact of exchangeable cations of Ca^{2+}, Mg^{2+}, Na^{+}, K^{+} on segregation of ice lenses when cooling down the soil monolith from the Source Clay Repository (Purdue University, West Lafayette, IN) and non-uniform soil from the Copper River Basin. It is found that the soils containing illite-smectite show no variation in their heaving properties as affected by Ca^{2+} and Na^{+} cations.

For the purpose of monitoring of irregular pavement surface displacement on the selected 15 m long sections the points were fixed with impact anchors and marked. The scheme of points' location was taken from the study [27] and is presented in Fig. 4. Due to reducing the cross section from 3 to 1.5 m the number of points per section was increased from 42 to 77. Leveling of the pavement had been performed in summer before freezing of the road structure and till the end of winter season, when stable positive temperatures were set.

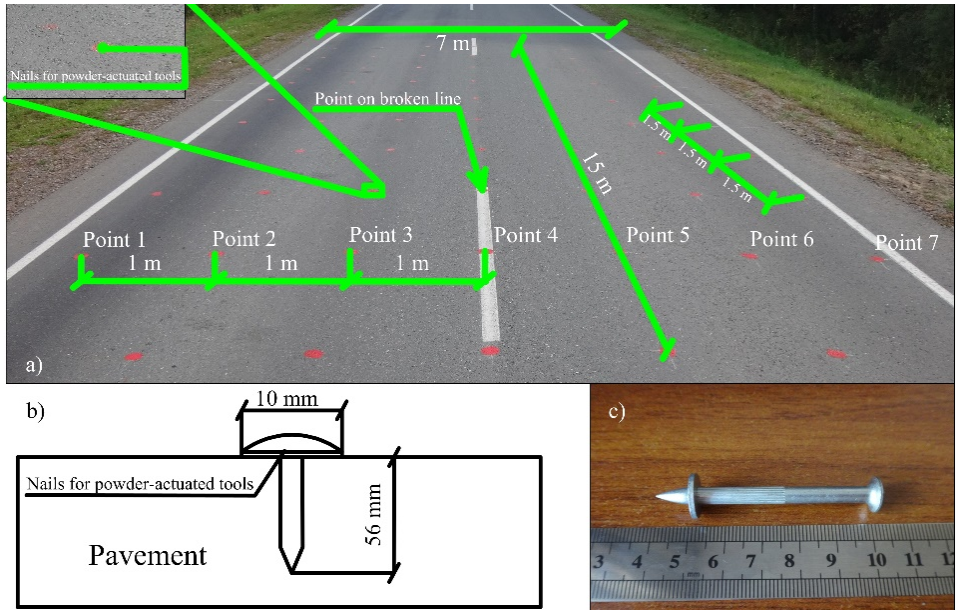

Figure 4. a) Scheme of points' location in the sections for monitoring of pavement surface displacement. b) Layout of the nail location in the pavement. c) Visual representation of the nail.

To ensure stability of marking when soil freezing and heaving occur, permanent reference markers were installed, in relation to which the points in the monitored section were leveled (Fig. 5). The permanent reference markers were covered with plastic caps to avoid moisture.

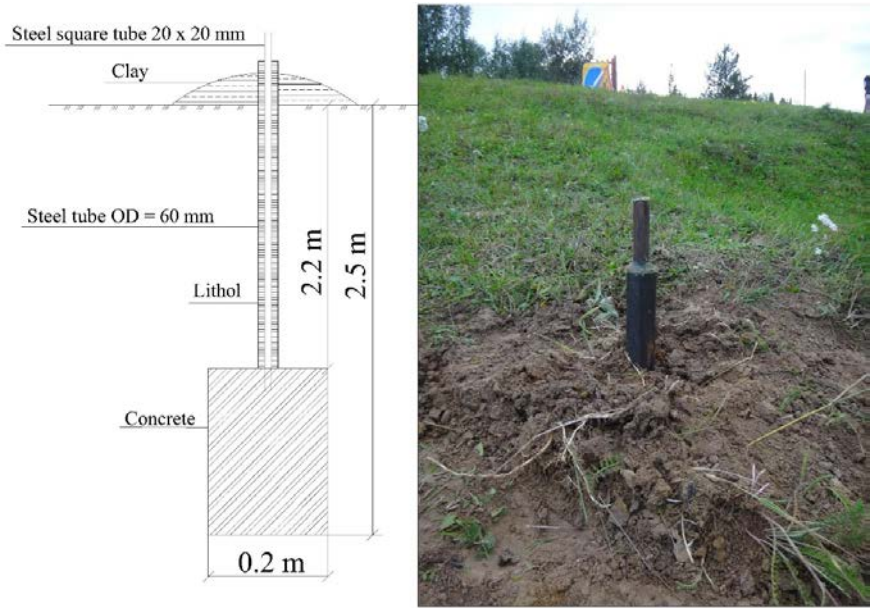

Figure 5. Permanent reference marker.

The results of surface irregular displacements analyzed in this study were obtained for 2017–2019 winter seasons. For instance, the average monthly air temperature during the winter season 2017–2018 for the sections No. 4 – 6 (south of the monitored region) was –10. 3 °C, while for the sections No. 13 – 14 (north of the monitored region) it was around –12.7 °C.

In many practical problems linear regression with a single regressor provides incomplete information on the independent variable [28, 29]. Frost heaving is affected by an array of factors, thus for building a prediction for an average roadway cross section is it preferable to use a multiple nonlinear regression model with a combination of factors. On the first stage, a nonlinear regression analysis of the vertical displacement

of pavement surface points on the broken line shall be performed for the selected road sections. A database with the parameters and values under study was created using Statistica software (Fig. 6). This model includes parameters available for engineers and serves as a rather quick solution with a satisfactory accuracy of result. The analyzed database can be found in the appendix to the paper in the "Table1" tab. Average variation of point displacements is found as the mean value for 7 points on the pavement within 1 section (Fig. 4).

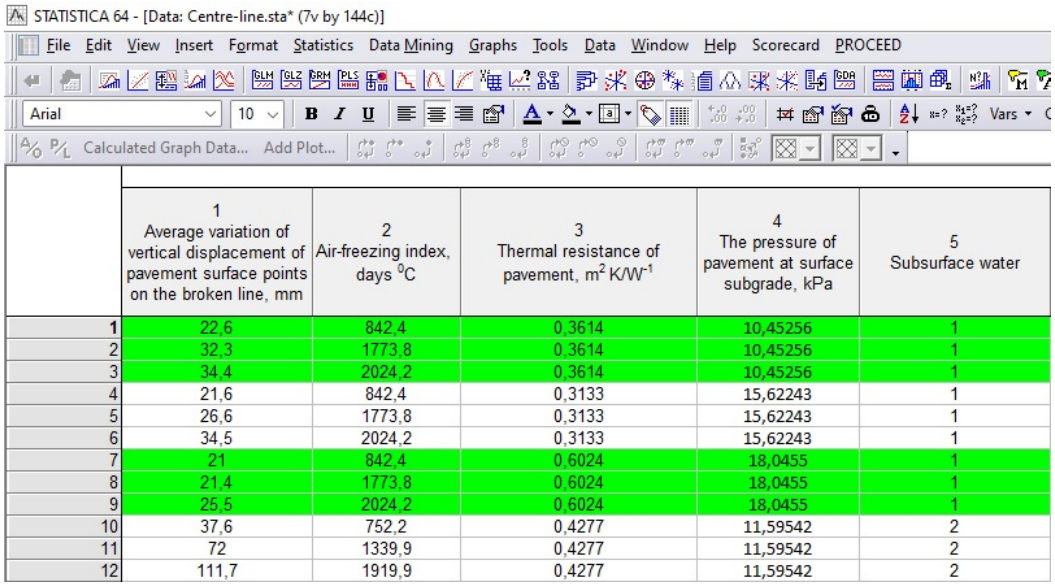

	1 Average variation of vertical displacement of pavement surface points on the broken line, mm	2 Air-freezing index, days ^{0}C	3 Thermal resistance of pavement, m^2 K/W^{-1}	4 The pressure of pavement at surface subgrade, kPa	5 Subsurface water
1	22,6	842,4	0,3614	10,45256	1
2	32,3	1773,8	0,3614	10,45256	1
3	34,4	2024,2	0,3614	10,45256	1
4	21,6	842,4	0,3133	15,62243	1
5	26,6	1773,8	0,3133	15,62243	1
6	34,5	2024,2	0,3133	15,62243	1
7	21	842,4	0,6024	18,0455	1
8	21,4	1773,8	0,6024	18,0455	1
9	25,5	2024,2	0,6024	18,0455	1
10	37,6	752,2	0,4277	11,59542	2
11	72	1339,9	0,4277	11,59542	2
12	111,7	1919,9	0,4277	11,59542	2

Figure 6. Statistica workspace with data for the parameters under study.

Air-freezing index $\left(\mathrm{FI}\right)$ is defined by the formula below [30]:

$$FI = \sum_{i=1}^{n} \overline{T}_i, \tag{1}$$

where $\overline{T}_i$ is average daily air temperature, °C.

Thermal resistance of pavement $\left(R_{\max}\right)$ is calculated using the following formula [31]:

$$R_{\max} = \sum_{i=1}^{n} \frac{z_i}{\lambda_i}, \tag{2}$$

where z_i is layer thickness, λ_i is thermal conductivity of pavement layer.

The pressure of pavement on the subgrade surface $\left(P\right)$ is defined by the formula below:

$$P = \frac{\sum_{i=1}^{n} m_i g}{S}, \tag{3}$$

where m_i is mass of the i^{th} structural layer of pavement, kg; g is gravitational acceleration, m/s^2; S is area of the subgrade surface subjected to pressure of pavement, m^2.

The impact of subsurface water is represented by a nominal scale. Value 2 in column 4 (Fig. 6) indicates that capillary rise of subsurface water has the effect on the value of frost heaving, while value 1 indicates zero effect.

The impact of subsurface water on frost heaving is evaluated based on its possible capillary rise to the freezing front [32]:

$$h_c = \frac{C}{e \cdot D_{10}}, \tag{4}$$

where C is constant (0.1 to 0.5 cm^2), e is void ratio, D_{10} is soil particle size, 10 percent finer passing (cm).

To predict the average variation of vertical displacement of pavement surface points on the broken line, 3 nonlinear regression models were built. The process of such model generation is given below.

A standard form of a multiple nonlinear regression model [28] is as follows:

$$E\left(Y\left|x_1,\ x_2,\ \ldots,\ x_k\right.\right)=\alpha_0+\beta_1x_1+\beta_2x_2+\beta_3x_3, \tag{5}$$

where Y is average variation of vertical displacement of pavement surface points on the broken line, α_0 is intercept, x_1 is air-freezing index, x_2 is thermal resistance of pavement, x_3 is subsurface water.

The average variation of vertical displacement of pavement surface points on the broken line is a dependent variable. The matrix elements are found by using the values of the studied parameters (air-freezing index, thermal resistance of pavement, subsurface water) in the formulas 6 – 8 [28]:

$$\begin{aligned} B_1a_{11}+B_2a_{12}+\ldots+B_ka_{1k}&=a_{1Y},\\ B_1a_{21}+B_2a_{22}+\ldots+B_ka_{2k}&=a_{2Y},\\ B_1a_{k1}+B_2a_{k2}+\ldots+B_ka_{kk}&=a_{kY}, \end{aligned} \tag{6}$$

$$a_{jj'}=\sum_j\left(x_{ij}-\overline{x}_i\right)\left(x_{j'j}-\overline{x}_{j'}\right)=a_{j'j}. \tag{7}$$

$$a_{jY}=\sum_j\left(x_{ij}-\overline{x}_i\right)\left(Y_j-\overline{Y}\right). \tag{8}$$

3. Results and Discussion

Calculation of formulas 6–8 is performed automatically with Statistica software for defining the matrix elements. Estimates obtained by using the least squares method for α_0, β_1, β_2, β_3, as well as the model parameters are presented in Table 3.

Table 3. Regression summary for the dependent variable.

	Standardized coefficients, β^*	Standard error of β^*	Partial regression coefficients, β	Standard error of β	t (52)	p-value
intercept			–0.00057	0.612979	–0.00093	0.99
x_1	0.375560	0.068740	1.06749	0.195386	5.46348	0.0000
x_2	–0.163756	0.069773	–3.70842	1.580082	–2.34698	0.0228
x_3	0.740057	0.069768	2.66608	0.251343	10.60733	0.0000

In Table 3, student's t-test for intercept is smaller than the threshold value based on the p-value that is bigger than 0.05. Hence, the hypothesis that the intercept is insignificant is accepted, and in the model it equals to zero. In Table 4, the model parameters are given for intercept = 0.

Table 4. Regression summary for the dependent variable (intercept = 0).

	Standardized coefficients, β^*	**Standard error of β^***	**Partial regression coefficients, β**	**Standard error of β**	**t (52)**	**p-value**
x₁	0.900947	0.018198	1.06731	0.021558	49.50866	0.0000
x₂	–0.032963	0.013861	–3.70854	1.559512	–2.37801	0.0210
x₃	0.156328	0.014546	2.66606	0.248071	10.74716	0.0000

In Table 4, the p-value is smaller than 0.05, and the hypothesis of significance of the factors in the model is accepted. Next, the normal probability plot of residuals is built (Fig. 7).

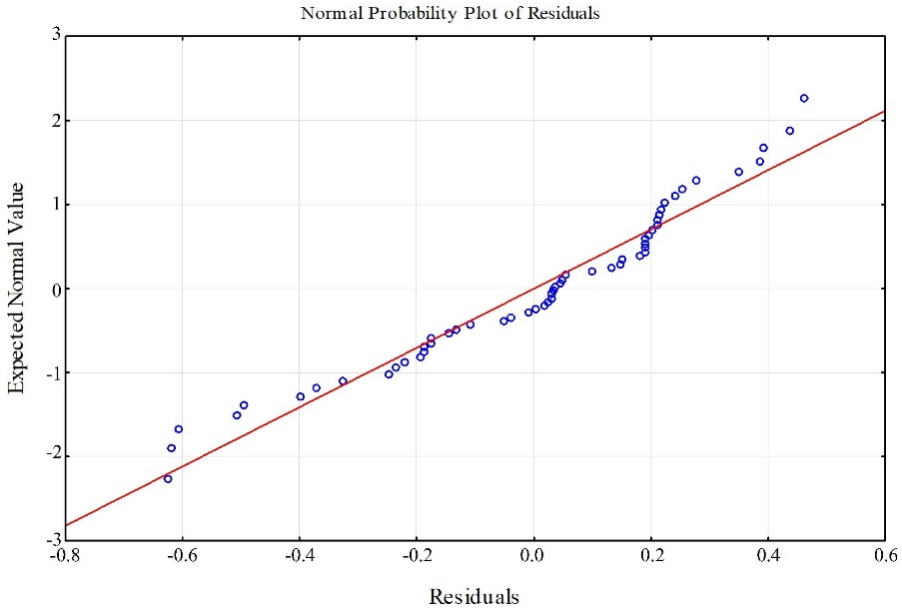

Figure 7. Normal probability plot of residuals.

On the plot (Fig. 7), no systematic deviations of actual observation data from the theoretical normal line are observed. Therefore, regression residuals follow the normal distribution. It should be defined whether there is a dependence of regression residuals on the predicted values (Fig. 8).

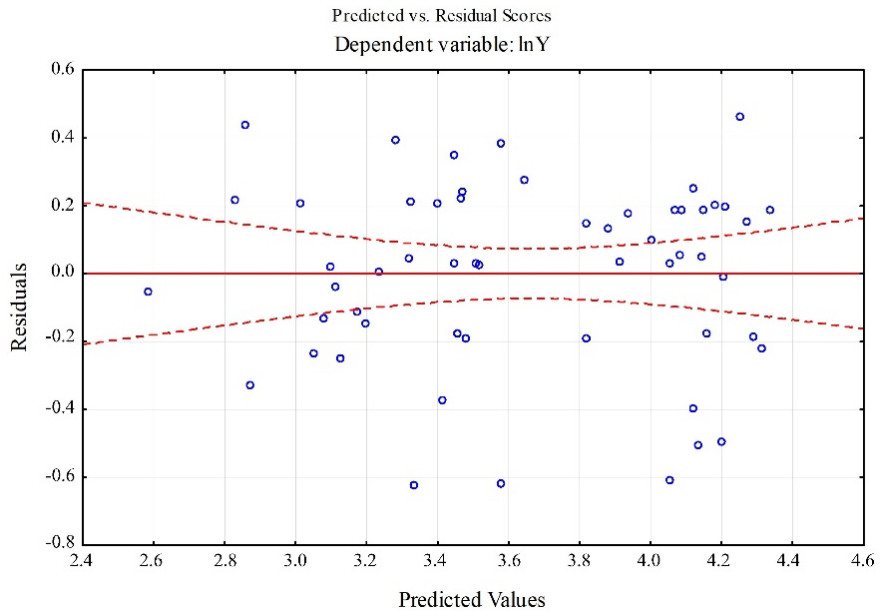

Figure 8. Plot of predicted vs. residual scores (0.95 conf. int.).

In the plot (Fig. 8), the dots are located chaotically, which means that the regression residuals are independent on the predicted values. Having fulfilled the condition of applicability of the obtained model [29], a comparison of dispersion caused by the difference between the groups with that caused by intra-class variance is presented in the following (Table 5).

Table 5. Analysis of variance.

Effect	Sums of squares	df	Mean squares	F	p-value
Regress.	760.3003	3	253.4334	3325.382	0.00
Residual	4.0392	53	0.0761		
Total	764.3395				

As seen from Table 5, the significance level for the regression model is smaller than 0.05, which indicates that the model is acceptable, and the average displacement of points on the broken line caused by frost heaving can be calculated as follows:

$$Y = \exp\left(1.06731 \cdot \log\left(FI\right) - 3.70854 \cdot R_{\max}^{5} + 2.66606 \cdot \log\left(SW\right)\right), \quad (9)$$

where Y is average variation of vertical displacement of pavement surface points on the broken line, mm; FI is air-freezing index, days °C; $R_{\max}$ is thermal resistance of pavement, m² K/W⁻¹; SW is the impact of subsurface water on frost heaving (2 – affects, 1 – does not affect).

As a result of statistical analysis of the data, two additional models of average variation of vertical displacement of pavement surface points on the broken line are built:

$$Y^{1} = 10^{\left(1.209602+0.167\cdot10^{-3}\cdot\left(FI\right)-0.60945\cdot10^{-7}\cdot P^{5}+0.496961\cdot\ln\left(SW\right)\right)}, \quad (10)$$

where Y^{1} is average variation of vertical displacement of pavement surface points on the broken line, mm; FI is air-freezing index, days °C; P is the pressure of pavement on the subgrade surface, kPa; SW is the impact of subsurface water on frost heaving (2 – affects, 1 – does not affect).

$$Y^{2} = -99.8766 \cdot 40.5205\log\left(FI\right) + 114.8265 \cdot \left(SW\right), \quad (11)$$

where Y^{2} is average variation of vertical displacement of pavement surface points on the broken line, mm; FI is air-freezing index, days °C; SW is the impact of subsurface water on frost heaving (2 – affects, 1 – does not affect).

The obtained models were checked for adequacy with the use of the results of vertical displacement of pavement surface points during the winter season 2019–2020. The monitoring results for these (test) roadway sections were not included when building the above models. The test sections' parameters and geolocations are given in the "Table 3 (test)" tab of the appendix to the paper.

Fig. 9 illustrates the results of comparison between the prediction for models $\left(Y,\ Y^{1},\ Y^{2}\right)$ and the 2019–2020 monitoring data. The detailed performance metrics for these prediction models are given in Table 6.

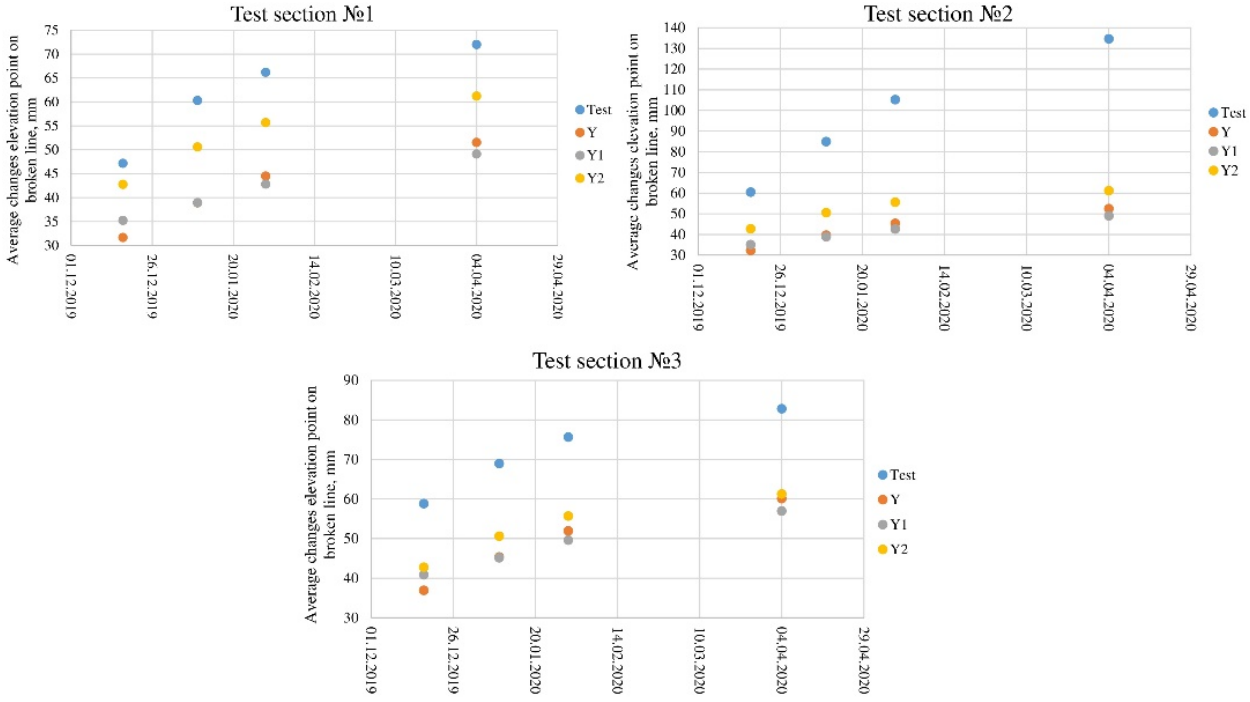

Figure 9. Results of comparison between the prediction and the monitoring data for test roadway sections.

Table 6. Performance metrics for the models of average variation of vertical displacement of pavement surface points on the broken line.

Models	Test section No. 1		Test section No. 2		Test section No. 3	
	MAE	RMSE	MAE	RMSE	MAE	RMSE
Y	19.768	19.923	53.870	57.391	23.002	23.014
Y^1	19.883	20.417	54.903	59.190	43.785	23.647
Y^2	8.835	9.202	43.785	48.344	18.992	19.101

Fig. 9 demonstrates the advantage of Y^2 alternative model. The prediction of time series of average variation of vertical displacement of pavement surface points on the broken line was performed for 3 test sections (Table 6) for which the measured data on pavement vertical displacement were obtained. MAE and RMSE are calculated as follows:

$$MAE = \frac{\left|\left(y_i - y_p\right)\right|}{n}, \tag{12}$$

$$RMSE = \sqrt{\frac{\sum\left(y_i - y_p\right)}{n}}, \tag{13}$$

where y_i is actual value; y_p is predicted value; n is number of observations.

In the meantime, MAE and $RMSE$ metrics of Y^2 model in all cases are found to be lower than those of the models Y and Y^1. Reduction of model factors had a positive effect. However, all three models showed unsatisfactory results for the test section No. 2. This can be explained either by an insufficient amount of monitoring data for the sections with close subsurface water occurrence, or by the fact that SW factor had its strong impact on the regression model coefficient calculation. It may be worth splitting the SW factor for close occurrence of subsurface water into levels as it approaches the pavement bottom, which is highlighted in the studies by Dahu [30] and Wang [31]. The value of subsurface water occurrence level for the test section No. 2 was the closest to the pavement bottom and was approximately equal to 180 cm. The general trend line of displacement of test section points coincides with the predicted model values with some error.

Based on the average vertical displacement of pavement surface points on the broken line caused by frost heaving let us define the relation of displacement of other points of the roadway cross section (points 1 – 6, Fig. 4). For that purpose, a database of the studied parameters was created (Fig. 10).

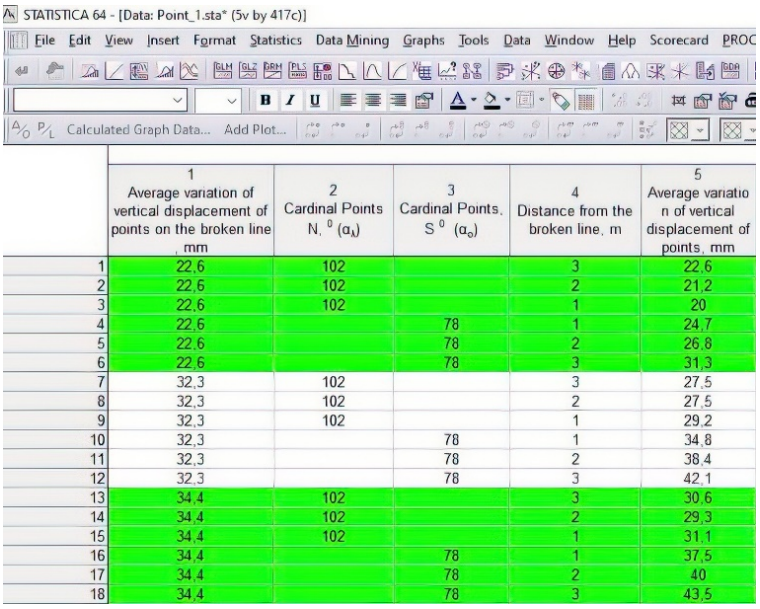
STATISTICA 64 - [Data: Point_1.sta* (5v by 417c)]

File Edit View Insert Format Statistics Data Mining Graphs Tools Data Window Help Scorecard PROC

Calculated Graph Data... Add Plot...

	1 Average variation of vertical displacement of points on the broken line, mm	2 Cardinal Points N, ^{0} (α_N)	3 Cardinal Points, S ^{0} (α_o)	4 Distance from the broken line, m	5 Average variation of vertical displacement of points, mm
1	22,6	102		3	22,6
2	22,6	102		2	21,2
3	22,6	102		1	20
4	22,6		78	1	24,7
5	22,6		78	2	26,8
6	22,6		78	3	31,3
7	32,3	102		3	27,5
8	32,3	102		2	27,5
9	32,3	102		1	29,2
10	32,3		78	1	34,8
11	32,3		78	2	38,4
12	32,3		78	3	42,1
13	34,4	102		3	30,6
14	34,4	102		2	29,3
15	34,4	102		1	31,1
16	34,4		78	1	37,5
17	34,4		78	2	40
18	34,4		78	3	43,5

Figure 10. Statistica workspace with the data for the parameters under study (for points 1 – 6, Fig. 4).

Right and left sides of the roadway cross section are defined in the direction of travel from West to East. Angles α_l and α_r are measured in degrees clockwise between the North direction and the centerline of the road for the left side of the roadway cross section, and counterclockwise between the South direction and the centerline of the road for the right side. The scheme of setting cardinal points for the Northern Hemisphere is given in Fig. 11.

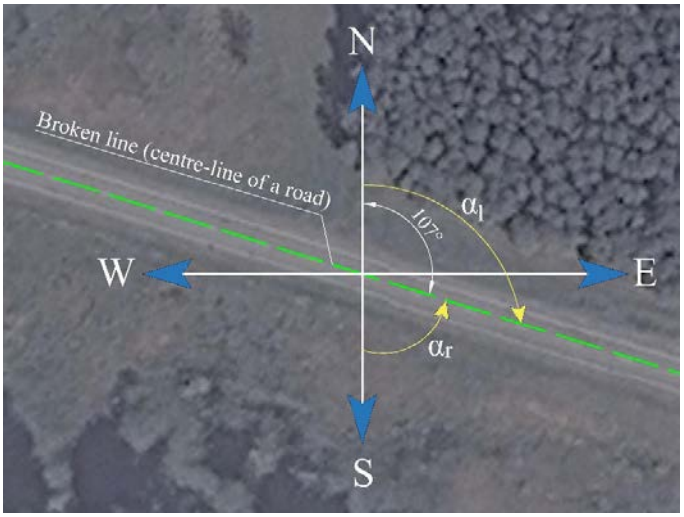

Figure 11. The scheme of setting cardinal points for the Northern Hemisphere.

The model parameters of the points displacement caused by frost heaving are given in Table 7 – for the left roadway cross section, and in Table 8 – for the right roadway cross section.

Table 7. Regression summary for the dependent variable (left roadway cross section).

	Standardized coefficients, β^*	Standard error of β^*	Partial regression coefficients, β	Standard error of β	*t* (164)	p-value
intercept			–3.73374	1.194798	–3.12500	0.002103
Y	0.973793	0.014314	1.00698	0.014801	68.03256	0.000000
Distance from the broken line	0.061105	0.014165	1.80357	0.418091	4.31383	0.000028
Cardinal point, α_l	0.046246	0.014314	0.00016	0.000049	3.23091	0.001491

Table 8. Regression summary for the dependent variable (right roadway cross section).

	Standardized coefficients, β^*	Standard error of β^*	Partial regression coefficients, β	Standard error of β	*t* (164)	p-value
Y	1.276508	0.033510	89.874	2.35930	38.09377	0.000000
Distance from the broken line	–0.299438	0.034991	–483.060	56.44889	–8.55747	0.000000
Cardinal point, α_r	–0.129914	0.027476	–0.043	0.00920	–4.72830	0.000005

In Table 7 and Table 8, the p-value is smaller than 0.05, which supports the hypothesis of significance of factors in the model of roadway cross section points displacement under the action of frost heaving. When performing statistical analysis of the model of points displacement for the right roadway cross section, the parameter of intercept was assumed equal to zero. Table 8 presents the results with intercept = 0.

The results of the analysis of variance (ANOVA) for the displacement model for the left and right roadway cross sections are given in Table 9 and Table 10, respectively.

Table 9. Analysis of variance (left roadway cross section).

Effect	Sums of squares	*df*	Mean squares	*F*	p-value
Regress.	94362.62	3	31454.21	1606.644	0.00
Residual	3210.72	164	19.58		
Total	97573.34				

Table 10. Analysis of variance (right roadway cross section).

Effect	Sums of squares	*df*	Mean squares	*F*	p-value
Regress.	1.921838E+09	3	640612566	891.9153	0.00
Residual	1.185102E+08	166	718244		
Total	2.040348E+09				

In Table 9 and Table 10, the F-test for the models of vertical displacement of pavement surface points is higher than the table values for 0.05 significance level considering the p-value parameter. Therefore, the hypothesis of factor significance is accepted and the vertical displacement of roadway cross section points can be calculated as follows:

$$Y_l = -3.73374 + 1.00698 \cdot Y + 1.80357 \cdot 1 + 0.00016 \cdot CP^2, \quad (14)$$

$$Y_r = \sqrt{89.874 \cdot Y - 483.060 \cdot 1 - 0.043 \cdot CP^2}, \quad (15)$$

where Y_l, Y_r are average variations of displacement of points (left and right sides of the roadway cross section), mm; Y is average variation of displacement of points on the broken line, mm; l is distance from the broken line, m; CP is cardinal points, deg.

Fig. 12 presents the comparison of results for the (Y_l, Y_r) model prediction and the 2019–2020 monitoring data. The dataset for the adequacy check for the regression model is given in the appendix to the paper in the "Table 3 (test)" tab. Detailed performance metrics for these prediction models for the test set are compiled in Table 11.

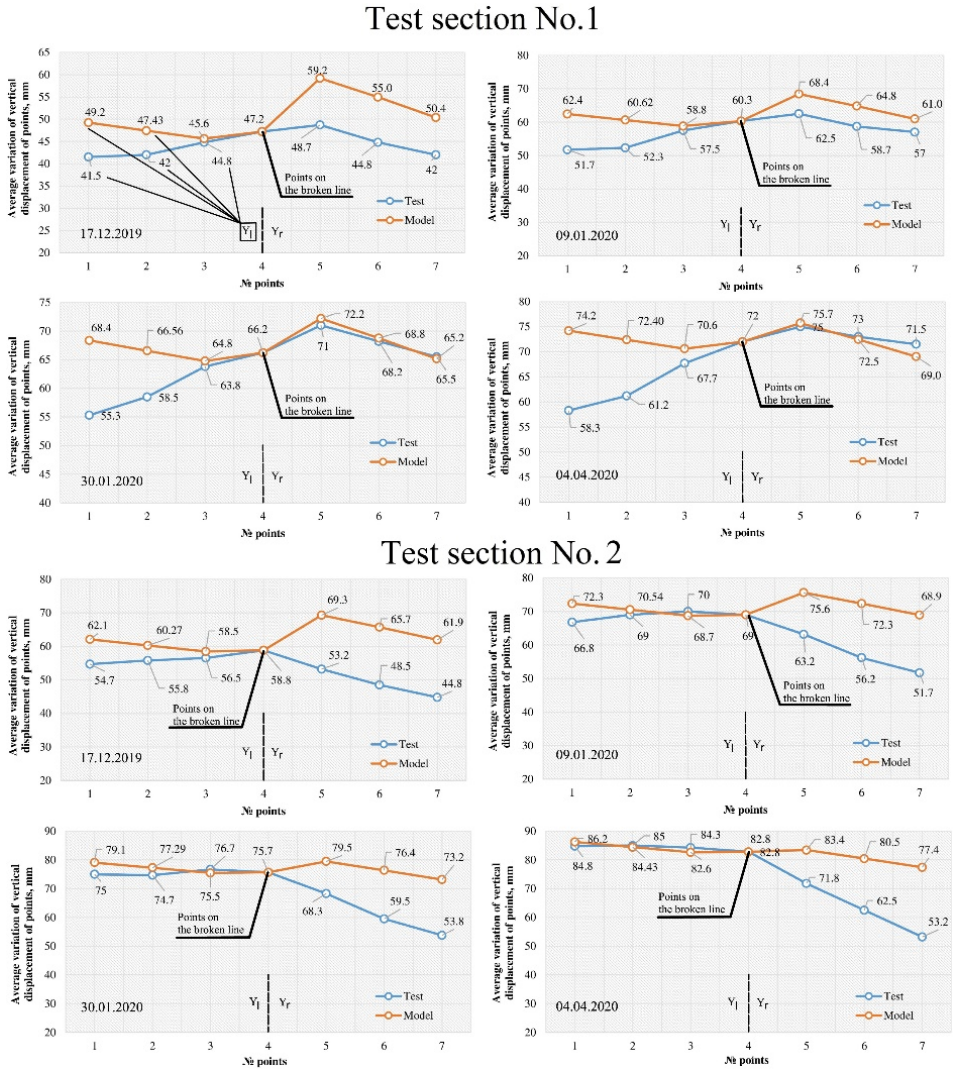

Figure 12. Comparison of the results for the (Y_l, Y_r) model prediction and the monitoring data for test sections (point №4 is located on the broken line).

Table 11. Performance metrics for the models (Y_l, Y_r).

Models	**Test sections No. 1, 3**	
	MAE	RMSE
Y_l	5.007	5.591
Y_l	Predicted Y	The residual
	43.2	–1.7
	41.3	0.7
	39.3	5.5
	57.4	–5.7
	55.5	–3.2
	53.5	4.0
	63.8	–8.5
	61.9	–3.4
	59.9	3.9
	70.1	–11.8
	68.2	–7.0
	66.2	1.5
	57.0	–2.3
	55.1	0.7
	53.2	3.3
	68.1	–1.3
	66.2	2.8
	64.2	5.8
	75.4	–0.4
	73.4	1.3
	71.5	5.2
	83.1	1.7
	81.1	3.9
	79.2	5.1
	MAE	RMSE
Y_r	10.345	12.533
Y_r	Predicted Y	The residual
	43.2	–1.7
	41.3	0.7
	39.3	5.5
	57.4	–5.7
	55.5	–3.2
	53.5	4.0
	63.8	–8.5
	61.9	–3.4
	59.9	3.9
	70.1	–11.8
	68.2	–7.0
	66.2	1.5
	57.0	–2.3
	55.1	0.7
	53.2	3.3
	68.1	–1.3
	66.2	2.8
	64.2	5.8
	75.4	–0.4
	73.4	1.3
	71.5	5.2
	83.1	1.7
	81.1	3.9
	79.2	5.1

In Fig. 12, the displacement prediction for points 1–3 is carried out by the Y_l model, and the Y_r model is used for points 5 – 7. Point 4 denotes the point on the broken line, and the value of its displacement was set based on the monitoring data. According to Fig. 12, for the test section No. 1 the predicted values for the left part of the pavement surface cross section are higher than those obtained in the process of monitoring. The same pattern is observed for the right part of the pavement cross section of the test section No. 3. This part and the left part of the section No. 1 are located in the embankment and have approximately the same moisture conditions. Also, it shall be taken into account that the right part of the cross section of the test section No. 1 is located in the open cutting. The left part of the test section No. 3 has additional inflow of moisture from the swampy side. Consequently, the models $\left(Y_l,\ Y_r\right)$ fit well for predicting mean displacement of pavement surface points in crosswise direction with moisture inflow. Table 11 demonstrates good convergence of the models $\left(Y_l,\ Y_r\right)$. To increase their efficiency it is suggested to differentiate between the moisture conditions of the roadway cross section (whether there is a moisture inflow to the freezing front). The left and the right parts of the roadway cross section may differ with respect to the conditions of moisture inflow to the freezing front. This shall be noted when designing roads on rough terrain.

After performing calculations of the equation 11 first, and then of the equations 14–15, the values of average vertical displacement of the roadway cross section under the action of frost heaving can be obtained. The risk of defects that may occur on the road pavement under irregular vertical displacement, the values of which were obtained after calculation of equations 11, 14–15, can be evaluated using the [32] mathematical model or specified software based on the final element method (FEM).

4. Conclusions

The models of irregular vertical displacement of pavement surface points, which were based on a thorough mathematical analysis, were found to be able to design an average pavement cross section of 15 m. When evaluating performance of the regression model of displacement of points on the broken line, an increase in the model accuracy was observed with a reduction of the number of factors. The best-performing RMSE value of the regression model $\left(Y^2\right)$ for prediction of mean displacement of points on the broken line was around 30 % when averaged over the test sections. The regression model of displacement of points on the broken line has satisfactory accuracy and requires further monitoring for its calibration. It is worth noting that the displacement trend for the three regression models $\left(Y,\ Y^1,\ Y^2\right)$ quite accurately accounts for the variation of displacement of pavement surface points in time with varying factors. In order to refine the prediction of mean displacements of pavement surface on the broken line caused by frost heave, the SW factor might be transformed from the nominal scale to the ordinal one. The SW factor has a significant impact on the prediction of irregular displacement of pavement surface points. Thus, when making a prediction of mean displacements of the pavement surface, one should refer to the least favorable conditions for the road section in question. The factors of the model of pavement displacement caused by frost heaving can be easily calculated by design engineers without additional complex and expensive tests. Good convergence was demonstrated by the models $\left(Y_l,\ Y_r\right)$ of mean irregular displacements of pavement surface points in crosswise direction for the sections where moisture migration to the freezing front is observed. The consideration of the angle of the roadway position relative to the North and South for predicting mean displacement of pavement surface points had a positive impact. Regression models of mean pavement displacements can be applied for evaluating frost resistance of pavement with asphalt concrete layers. This approach enables consideration of the solution to the issue of subgrade frost heave from top to bottom. Having defined the value of pavement surface points displacement one can assume what amount of ice the roadway subgrade clay contains. The model is applicable to evaluate evenness of road pavement affected by frost heave.

The model is based on empirical results, which can limit its applicability for different pavement freezing conditions. Another limitation of the model is a pavement width of 8 meters. To make predictions for wider sections, similar research is required to calibrate the model. The suggested model is not applicable for predicting average irregular vertical displacements occurring in sand-clay soils, where freezing and heaving processes differ from those in clay soils.

5. Data Availability

Some or all data, models, or code that support the findings of this study are available from the corresponding author upon reasonable request.

Churilin, V.S. 2021. "Data of irregular vertical displacement of a roadway cross section caused by frost heaving" Harvard Dataverse Accessed September 14, 2021. https://doi.org/10.7910/DVN/DBZ92O

References

1. Kottek, M., Grieser, J., Beck, C., Rudolf, B., Rubel, F. World Map of Köppen-Geiger Climate Classification updated. Meteorologische Zeitschrift. 2006. 15. Pp. 259–263. DOI: 10.1127/0941-2948/2006/0130
2. Jin, H., Wei, Z., Wang, S., Yu, Q., Lu, L., Wu, Q., Ji, Y. Assessment of frozen-ground conditions for engineering geology along the Qinghai–Tibet highway and railway, China. Engineering Geology. 2008. DOI: 10.1016/j.enggeo.2008.04.001
3. Dagli, D. Laboratory investigations of frost action mechanisms in soils. Diss. Luleå Tekniska Universitet, 2017.
4. Ivanov, K.S. Granulated foam-glass ceramics for ground protection against freezing. Magazine of Civil Engineering. 2018. 79(3). Pp. 95–102. DOI: 10.18720/MCE.79.10
5. Taber, S. The mechanics of frost heaving. The Journal of Geology. 1930. 38(4). Pp. 307–317. DOI: 10.1086/623720
6. Beskow, G. Soil freezing and frost heaving, with special application to roads and railroads. Swedish Geological Society, Series C (375). (translated by J.O. Osterberg). Historical Perspectives in Frost Heave Research. 1935. Pp. 41–157 CRREL. Special Report. Pp. 91–23.
7. Tsytovich, N. Osnovaniya i fundamenty na merzlykh gruntakh [Bases and foundations on frozen soil]. National Academy of Sciences, National Research Council, 1958. 168 p. (rus)
8. Feng, R., Wu, L., Wang, B. Numerical Simulation for Temperature Field and Salt Heave Influential Depth Estimation in Sulfate Saline Soil Highway Foundations. International Journal of Geomechanics. 2020. 20(10). DOI: 10.1061/(ASCE)GM.1943-5622.0001843
9. Zhang, X., Zhai, E., Wu, Y., Sun, D., Lu, Y. Theoretical and Numerical Analyses on Hydro–Thermal–Salt–Mechanical Interaction of Unsaturated Salinized Soil Subjected to Typical Unidirectional Freezing Process. International Journal of Geomechanics. 2021. 21(7). DOI: 10.1061/(ASCE)GM.1943-5622.0002036
10. Black, P.B., Hardenberg, M.J. Historical Perspectives in Frost Heave Research The Early Works of S. Taber and G. Beskow. Hanover. New Hampshire: U.S. Army Corps of Engineers Cold Regions Research & Engineering Laboratory, 1991. 167 p.
11. Puzakov, N. Vodno-teplovoy rezhim gruntovogo pokrytiya avtomobil'nykh dorog [Water and heat regime of road subgrade]. Moscow: Avtotransizdat, 1958. 168 p. (rus)
12. Penner, E. The importance of freezing rate in frost action in soils. Proceedings of the American Society for Testing and Materials. 1960. 60. Pp. 1151–1165.
13. O'Neill, K., Miller, R.D. Explorations of a rigid ice model of frost heave. Water Resour. Res. 1985. 21(3). Pp. 281–296. DOI: 10.1029/WR021i003p00281
14. Liu, Z., Yu, X. Coupled thermo-hydro-mechanical model for porous materials under frost action: theory and implementation. Acta Geotechnica. 2011. DOI: 10.1007/s11440-011-0135-6
15. Hao, Z., Shunji, K., Fujun, N., Anyuan, L. Three-dimensional frost heave evaluation based on practical Takashi's equation. Cold Regions Science and Technology. 2015. 118. Pp. 30–37. DOI: 10.1016/j.coldregions.2015.06.010
16. Teng, J., Liu, J., Zhang, S., Sheng, D. Modelling frost heave in unsaturated coarse-grained soils. Acta Geotechnica. 2020. 15. Pp. 3307–3320. DOI: 10.1007/s11440-020-00956-2
17. Huang, S., Lu, Z., Ye, Z., Xin, Z. An elastoplastic model of frost deformation for the porous rock under freeze-thaw. Engineering Geology. 2020. 278. 105820. DOI: 10.1016/j.enggeo.2020.105820
18. Jing, C., Anyuan. L., Chunyan, B., Yanhua, D., Minghao, L., Zhanju, L., Fujun, N., Tianxiang, Z. A deep learning forecasting method for frost heave deformation of high-speed railway subgrade. Cold Regions Science and Technology. 2021. 185. 103265. DOI: 10.1016/j.coldregions.2021.103265
19. Efimenko, V.N., Efimenko, S.V., Teltaev, B.B., Sukhorukov, A.V. On the need for differentiated account of properties of the geocomplex of territories in pavements design. News of the Academy of sciences of the Republic of Kazakhstan Satbayev University. Series of Geology and Technical Sciences. 2020. 2(440). Pp. 72–80. DOI: 10.32014/2020.2518-170X.33
20. ASTM D 2487 – 17 Standard Practice for Classification of Soils for Engineering Purposes (Unified Soil Classification System).
21. Interstate Standard GOST 5180 – 2015 Soils. Laboratory methods for determination of physical characteristics. 2016. 19 p.
22. ISO/TS 17892 – 12:2018 Geotechnical investigation and testing – Laboratory testing of soil – Part 12: Determination of liquid and plastic limits.
23. ISO 14688-2:2017 Geotechnical investigation and testing – Identification and classification of soil – Part 2: Principles for a classification.
24. GOST 28622 – 2012 Soils. Laboratory method for determination of frost-heave degree.
25. Efimenko, V.N., Vilisov, V.P., 1983. "Analiz prichin razrusheniya nezhyostkih dorozhnyh odezhd v usloviyah Zapadnoj Sibiri [Analysis of destruction of non-rigid pavements in West Siberia]." Racional'nye metody stroitel'stva i ehkspluatacii avtomobil'nyh dorog v usloviyah Sibiri. Tomsk. TSU Publ. Pp. 41–45. (rus)
26. Darrow, M.M., Ross, M.L. Visualizing cation treatment effects on frozen clay soils through μCT scanning. Cold Regions Science and Technology. 2020. 175. 103085. DOI: 10.1016/j.coldregions.2020.103085
27. Preferansova, L.A., Troitskaya, M.N., Bel'kovskij, S.V. Proektirovanie gruntovyh osnovanij usovershenstvovannyh pokrytij s uchjotom ih raboty v zimnih uslovijah [Design of soil bases for improved coatings, taking into account their work in winter conditions]. 1953. 113 p. (rus)
28. Johnson, N.L., Leone, F.C. Statistics and experimental design in engineering and the physical sciences. New York: Wiley, 1964. 534 p.

29. StatSoft, Inc. Electronic Statistics Textbook. Tulsa, OK: StatSoft. 2011. [Online] URL: http://www.statsoft.com/textbook (reference date: 06.11.2022)
30. Calculation Methods for Determination of Depths of Freeze and Thaw Soils – Emergency Construction. Department of the Air Force. Manual AFM 88-40. Chapter 46. Washington, D.C.
31. Stenberg, L. Design of frost protection in roads. Linköping: Statens Väg- och Trafikinstitut., VTI notat V 223. 1993.
32. Oman, M.S., Neil G.L., Braun, I. Designing base and subbase to resist environmental effects on pavements. No. MN/RC 2018-06. Minnesota. Dept. of Transportation. Research Services & Library. 2018.
33. Dahu, R., Jinbang, Z., Guoyu, L., Jun, Z., Teruyuki, S. Field experimental study of the characteristics of heat and water transfer during frost heaving. Cold Regions Science and Technology. 2019. 168. 102892. DOI: 10.1016/j.coldregions.2019.102892
34. Wang, T., Liu, Y., Wang, J., Wang, D. Assessment of spatial variability of hydraulic conductivity of seasonally frozen ground in Northeast China. Engineering Geology. 2020. 274. 105741. DOI: 10.1016/j.enggeo.2020.105741
35. Churilin, V., Efimenko, S., Matvienko, O., Bazuev, V. Simulation of stresses in asphalt-concrete pavement with frost heaving. MATEC Web of Conferences. 2018. 216. 01011. DOI: 10.1051/matecconf/201821601011

Information about authors:

Vladimir Churilin, *PhD in Technical Sciences*
ORCID: https://orcid.org/0000-0002-8898-4766
E-mail: lex-16-2008@mail.ru

Oleg Matvienko, *Doctor of Physical and Mathematical Sciences*
E-mail: matvolegv@mail.ru

Vladimir Efimenko, *Doctor of Technical Sciences*
E-mail: svefimenko80@gmail.com

Sergei Efimenko, *Doctor of Technical Sciences*
E-mail: svefimenko_80@mail.ru

Received 06.11.2022. Approved after reviewing 09.01.2023. Accepted 15.01.2023.